Predicting leptomeningeal disease spread after resection of brain metastases using machine learning

Tewarie, I.A.; Senko, A.W.; Jessurun, C.A.C.; Zhang, A.T.; Hulsbergen, A.F.C.; Rendon, L.; ... ; Phillips, J.G.

JNS

CLINICAL ARTICLE

J Neurosurg 138:1561–1569, 2023

Predicting leptomeningeal disease spread after resection of brain metastases using machine learning

Ishaan Ashwini Tewarie, MD,[1–4] Alexander W. Senko, PhD,[1] Charissa A. C. Jessurun, MD,[1,3,4] Abigail Tianai Zhang, BS,[1] Alexander F. C. Hulsbergen, MD,[1,3,4] Luis Rendon, MD,[1] Jack McNulty, MD,[1] Marike L. D. Broekman, MD, PhD, LLM,[1,3,4] Luke C. Peng, MD, MS,[1] Timothy R. Smith, MD, PhD, MPH,[1] and John G. Phillips, MD, MPH[1,5]

[1]Department of Neurosurgery, Computational Neuroscience Outcomes Center, Brigham and Women's Hospital, Harvard Medical School, Boston, Massachusetts; [2]Faculty of Medicine, Erasmus University Rotterdam/Erasmus Medical Center, Rotterdam; [3]Department of Neurosurgery, Haaglanden Medical Center, The Hague; [4]Department of Neurosurgery, Leiden Medical Center, Leiden, The Netherlands; and [5]Department of Radiation Oncology, Tennessee Oncology, Nashville, Tennessee

OBJECTIVE The incidence of leptomeningeal disease (LMD) has increased as treatments for brain metastases (BMs) have improved and patients with metastatic disease are living longer. Sample sizes of individual studies investigating LMD after surgery for BMs and its risk factors have been limited, ranging from 200 to 400 patients at risk for LMD, which only allows the use of conventional biostatistics. Here, the authors used machine learning techniques to enhance LMD prediction in a cohort of surgically treated BMs.

METHODS A conditional survival forest, a Cox proportional hazards model, an extreme gradient boosting (XGBoost) classifier, an extra trees classifier, and logistic regression were trained. A synthetic minority oversampling technique (SMOTE) was used to train the models and handle the inherent class imbalance. Patients were divided into an 80:20 training and test set. Fivefold cross-validation was used on the training set for hyperparameter optimization. Patients eligible for study inclusion were adults who had consecutively undergone neurosurgical BM treatment, had been admitted to Brigham and Women's Hospital from January 2007 through December 2019, and had a minimum of 1 month of follow-up after neurosurgical treatment.

RESULTS A total of 1054 surgically treated BM patients were included in this analysis. LMD occurred in 168 patients (15.9%) at a median of 7.05 months after BM diagnosis. The discrimination of LMD occurrence was optimal using an XGboost algorithm (area under the curve = 0.83), and the time to LMD was prognosticated evenly by the random forest algorithm and the Cox proportional hazards model (C-index = 0.76). The most important feature for both LMD classification and regression was the BM proximity to the CSF space, followed by a cerebellar BM location. Lymph node metastasis of the primary tumor at BM diagnosis and a cerebellar BM location were the strongest risk factors for both LMD occurrence and time to LMD.

CONCLUSIONS The outcomes of LMD patients in the BM population are predictable using SMOTE and machine learning. Lymph node metastasis of the primary tumor at BM diagnosis and a cerebellar BM location were the strongest LMD risk factors.

https://thejns.org/doi/abs/10.3171/2022.8.JNS22744

KEYWORDS brain metastases; leptomeningeal disease; prediction models; risk factors; machine learning; oncology

The incidence of leptomeningeal disease (LMD) has increased as treatments for both primary malignancies and brain metastases (BMs) have improved. Despite the improvements in response and overall survival in many metastatic cancers, LMD remains relatively intractable to therapies and almost universally fatal.[1] LMD is thought to spread via the cerebrospinal fluid (CSF). Mechanical disruption of BMs during resection may lead to the extension of new metastases into the leptomeninges, causing LMD.[2] The intractability is partly due to the dif-

ABBREVIATIONS AUC = area under the curve; BM = brain metastasis; cLMD = classical/diffuse LMD; CSF = cerebrospinal fluid; CUSA = cavitron ultrasonic surgical aspirator; GTR = gross-total resection; HER2 = human epidermal growth factor receptor 2; LMD = leptomeningeal disease; LN = lymph node; ML = machine learning; nLMD = nodular LMD; PPI = proton pump inhibitor; SMOTE = synthetic minority oversampling technique; SRS = stereotactic radiosurgery; WBRT = whole-brain radiotherapy; XGBoost = extreme gradient boosting.

SUBMITTED March 29, 2022. **ACCEPTED** August 25, 2022.
INCLUDE WHEN CITING Published online October 21, 2022; DOI: 10.3171/2022.8.JNS22744.

ficulty of achieving high chemotherapy concentrations because of the blood-brain barrier or in safely treating the entire CSF space with tumoricidal doses. LMD is considered fatal even with optimal treatment, with a median survival of 2–4 months.[3–5] The current literature suggests that surgery can increase the incidence of LMD by tumor spillage into the CSF.[6–8] However, the sample sizes used in individual studies of LMD occurrence and its risk factors have been limited, ranging from 200 to 400 patients.

Machine learning (ML), a branch of artificial intelligence, is increasingly used in neuro-oncology for various applications such as predicting survival or detecting brain tumors at diagnosis and recurrence.[9–11] In the present study, we explored LMD risk factors and the ability of ML to enhance LMD prediction performance in a cohort of 1054 surgically treated BMs, the largest cohort reported to date in the literature, allowing for more thorough ML modeling.

Methods

Study Design and Participants

All patients eligible for study inclusion were adults who had consecutively undergone neurosurgical BM treatment, had been admitted to Brigham and Women's Hospital in Boston, Massachusetts, from January 2007 through December 2019, and had a minimum of 1 month of follow-up after neurosurgical treatment. Data in the Brigham and Women's Hospital were collected under Partners Healthcare institutional review board approval. Variables were retrospectively collected from the BM diagnosis onward, with the occurrence of and time to LMD as the primary outcomes. The cohort was first split into a training and testing set using a stratified 80/20 split so that each split contained the same proportion of LMD patients.

Outcome Variables

The primary outcome was the binary occurrence of LMD (yes/no) for classification models and the time from BM diagnosis to LMD for regression models. Where possible, LMD was ascertained on the basis of the cytological analysis of CSF combined with complete diagnostic workup. Cytological analysis was not always performed because of patient prognosis and quality-of-life concerns. Therefore, patients with the persistent presence of LMD on cerebrospinal MRI combined with clinical evaluations, as described in the LMD clinical practice guidelines,[12] were also included. LMD was further classified as either nodular (nLMD) or classical/diffuse (cLMD), defined as nodular enhancing lesions on leptomeninges and the classic sugarcoating pattern, respectively, based on MRI studies and radiology reports for further subanalyses.[13,14] The presence of LMD and the further subclassification thereof were independently assessed by three authors (A.T.Z., L.R., and J.M.) and subsequently assessed by either of two authors (I.A.T. or C.A.C.J.). The interobserver correlation between the first assessment and the subsequent assessment was measured using Cohen's kappa.[15]

Descriptive Variables

The following independent variables were collected: patient characteristics (age at BM diagnosis, sex, Karnofsky Performance Status at BM diagnosis, and neurological deficits), tumor characteristics (type of primary tumor, primary tumor spread at BM diagnosis, systemic disease status, BM location, hemorrhagic and cystic features of the resected BM, BM size defined as the largest dimension, number of BMs, and proximity to CSF space), and treatment characteristics (time from BM diagnosis to BM surgery, extent of resection, method of resection [piecemeal or en bloc], use of cavitron ultrasonic surgical aspirator [CUSA], ventricular violation during surgery, time from BM diagnosis to stereotactic radiosurgery [SRS], time to whole-brain radiotherapy [WBRT], prior WBRT or SRS, total dose of steroids at BM diagnosis, steroid tapering, and use of proton pump inhibitors [PPIs] at BM diagnosis). The primary tumor spread at BM diagnosis was noted using oncology codes, clinical reports, and accompanied imaging reports, including thorax-abdomen CT and PET-CT imaging. The use of CUSA was documented from billing records. Binary classification of BM location was used for the exploratory analyses and prediction models (i.e., supratentorial vs infratentorial location) since the current neurosurgical literature has demonstrated that lobar location is often biased, as tumors occur in a multilobed manner.[16] Extent of resection was defined according to the Response Assessment in Neuro-Oncology Brain Metastases criteria and assessed using volumetric analyses on pre- and postoperative MRI studies.[17] The method of BM resection was classified as either piecemeal or en bloc (defined as the circumferential removal of BMs with an intact tumor capsule), as described in the operative report. Ventricular violation during surgery was also extracted from operative reports and postoperative radiological reports. The resected BMs were classified with a cystic or hemorrhagic component based on the presence of such clinically relevant components, as indicated in the radiology reports. The primary malignancy status was defined as controlled if the primary malignancy did not demonstrate growth in the follow-up leading up to the BM diagnosis. Proximity to the CSF space, information collected from radiology reports, was classified as follows, according to the literature definition: 1) completely separated from the ventricles and pia mater and entirely surrounded by brain parenchyma, 2) metastasis adjacent to the ventricle walls or pia mater, and 3) involvement of metastasis with the CSF space with pial or ependymal enhancement.[3]

Sample Size

Our data set will have an inherent class imbalance; the minority class (i.e., the patients who developed LMD) will be underrepresented compared to BM patients with no LMD. Because of this imbalance, untuned ML models can have an erroneous tendency to predict the majority class, negatively impacting true predictive performance.[18] To address the imbalance, we utilized the synthetic minority oversampling technique (SMOTE), which uses a k-nearest neighbors algorithm to impute new patients in the minority and majority classes. The SMOTE ratio describes the final ratio of underrepresented/overrepresented classes after oversampling.[19]

Censoring

Patients were censored at the date of death if LMD did not occur. Patients who did not die or did not experience intracranial progression were censored at the date of the last follow-up known in the electronic health record. Data extraction of the outcome and dependent variables for LMD concluded in March 2021.

Statistical Analysis

The analysis was conducted using R version 4.0.3[20] (R Foundation for Statistical Computing) and Python version 3.6[21] (Python Software Foundation) using the PySurvival package and scikit-learn library.[22] Missing data were imputed for prediction modeling only, using the scikit-learn[22] library's IterativeImputer class, which implements a version of multivariate imputation. Complete patient cases were used to assess the predictability of LMD using traditional regression and classification models. Two regression models were trained—a conditional survival forest algorithm and a Cox proportional hazards algorithm—with time to LMD as the outcome. Three classification models—logistic regression, extra trees classifier, and extreme gradient boosting (XGBoost) algorithm—were explored with the binary occurrence of LMD as the outcome. Feature selection for prognostication was performed using a minimum redundancy–maximum relevance approach,[23] with a set number of input variables with respect to degrees of freedom, to discover potential new independent variables and explore what set of input variables would deliver the best LMD prognostication. Hyperparameter tuning was done via fivefold cross-validation on the training set. Performance was assessed using an area under the receiver operating characteristic curve for the classification task. The performance of the regression models was measured using the C-index. Calibration was assessed via reliability plots, which graphically express the difference between observed and predicted outcomes of LMD models on the hold-out test.[24]

Risk Factors for LMD: An Exploratory Analysis

Logistic regression and a Cox proportional hazards model were used to determine the statistical relationship between the strongest risk factors and (time to) LMD. The selected independent variables were based on expert knowledge and the current literature. The explored risk factors were as follows: extracranial metastases at BM diagnosis[25] categorized as intracranial BM, lymph node (LN) metastasis, solid organ metastasis, or LN and solid organ metastasis; BM location;[26–29] BM histology;[3,26,29–31] number of BMs;[27,32,33] cystic or hemorrhagic BMs;[33] proximity to CSF space;[3] extent of resection;[26,30] method of resection;[3,26,28,31,33] and time to adjuvant radiation.[26,27] Additionally, the era of treatment, divided into three periods (2007–2011, 2012–2016, and 2017–2019) was included in the final models to explore whether earlier eras of treatment were associated with an increased risk or hazard for LMD to account for the improvement in (adjuvant) BM treatment modalities in the inclusion period. Relative risk ratios (logistic regression) and hazard ratios (Cox proportional hazards model) were computed with the 95% confidence intervals. Kaplan-Meier survival curves were computed to visualize survival curves for the risk factors significantly associated with LMD. Subgroup analyses based on primary tumor histology were additionally performed. In these analyses, molecular features for breast and lung BMs (i.e., human epidermal growth factor receptor 2 [HER2], progesterone, estrogen, ALK, KRAS, EGFR, and PDL1 status) were included. Adjustment for multiple testing was performed using the Holm-Bonferroni method.

Results

Descriptive Analysis of All Surgically Treated BM Patients

A total of 1054 surgically treated BM patients were included in this analysis. The mean age was 60.8 years, and 57.5% of the patients (n = 606) were female. The median number of BMs observed at diagnosis was 2, and the median BM diameter was 31.57 mm. Two hundred two patients had received some form of CNS radiation: 100 (9.5%) WBRT and 102 (9.8%) SRS. Data on whether lesions treated with radiation were ultimately the resected lesion were limited. LMD occurred in 168 patients (15.9%) at a median of 7.05 months after BM diagnosis. Interobserver agreement was strong with a Cohen's kappa of 0.87 between the two independent assessments. Forty-nine patients (4.6%) had an nLMD pattern versus 119 patients (11.3%) who developed a cLMD pattern. Interobserver agreement for LMD type was deemed moderate with a Cohen's kappa of 0.74. The lower interobserver agreement for LMD type was due to its inherent qualitative assessment. The median time to surgery from first admittance in the health records was 6 days. The BMs originated from primary lung cancer (n = 481, 45.6%), breast cancer (n = 148, 14.0%), melanoma (n = 140, 13.3%), colorectal cancer (n = 21, 2.0%), gynecological cancer (n = 55, 5.2%), renal cancer (n = 50, 4.7%), and various tumor types classified as other (n = 159, 15.1%). At BM diagnosis, 478 patients (45.4%) had no systemic tumor spread other than the BM, 181 (17.2%) also had LN metastasis, 215 (20.4%) had extracranial metastases, and 180 (17.1%) had both LN metastasis and other solid organ metastases. Cystic BMs occurred in 296 patients (28.1%), whereas 406 patients (38.5%) had hemorrhagic BMs. The BMs occurred in a supratentorial location (n = 818, 77.6%) and an infratentorial location (n = 261, 24.8%); the lobar classification is summarized in Table 1. Sixty patients had a BM involved with CSF-carrying structures, and 213 had a BM adjacent to a CSF-carrying structure. Gross-total resection (GTR) was achieved in 940 patients (89.2%). Data were missing rarely and at random, with the exact time sequence to adjuvant WBRT reported as the most frequent missing variable, missing data for 14 patients (1.3%) treated with adjuvant WBRT and missing data on steroid dosage in 9 patients (0.9%). Additional characteristics regarding tumor, treatment, or the patient are summarized in Table 1.

Conventional Biostatistics: LMD Risk Factors

In the multivariate logistic regression, cerebral BM location (risk ratio [RR] 0.53, 95% CI 0.36–0.79, p = 0.001) was significantly associated with a decreased risk of LMD. GTR (RR 0.58, 95% CI 0.37–1.03, p = 0.048) demonstrat-

TABLE 1. Clinical characteristics of study cohort

Variable	Overall Cohort	LMD Cohort	Control Cohort
No. of patients (%)	1054 (100.0)	168 (15.9)	886 (84.1)
Mean age in yrs (SD)	60.8 (11.8)	57.13 (12.5)	61.47 (11.5)
Female sex, no. (%)	606 (57.5)	111 (66.1)	495 (55.9)
Primary tumor, no. (%)			
Lung cancer	481 (45.6)	72 (42.9)	409 (46.2)
Breast cancer	148 (14.0)	38 (22.6)	110 (12.4)
Melanoma	140 (13.3)	19 (11.3)	121 (13.7)
Colorectal cancer	21 (2.0)	5 (3.0)	16 (1.8)
Gynecological cancer	55 (5.2)	11 (6.5)	44 (5.0)
Renal cancer	50 (4.7)	3 (1.8)	47 (5.3)
Other	159 (15.1)	20 (11.9)	139 (15.7)
Median time from Dx to surgery in days	6.00	7.0	6.0
Primary tumor spread at BM Dx, no. (%)			
Intracranial only	478 (45.4)	58 (34.5)	420 (47.4)
LNs	181 (17.2)	47 (28.0)	134 (15.1)
Extracranial metastases	215 (20.4)	31 (18.5)	184 (20.8)
LNs & extracranial metastases	180 (17.1)	32 (19.0)	148 (16.7)
Systemic disease status, no. (%)			
Active	688 (65.3)	119 (70.8)	569 (64.2)
Controlled	366 (34.7)	49 (29.2)	317 (35.8)
Lobar classification, no. (%)			
Frontal	364 (34.5)	51 (30.5)	313 (35.3)
Parietal	230 (21.8)	27 (16.2)	203 (22.9)
Temporal	125 (11.9)	12 (7.2)	113 (12.8)
Occipital	99 (9.4)	16 (9.6)	83 (9.4)
Cerebellar	261 (24.8)	61 (36.5)	200 (22.6)
Median no. of BMs	2	2	
Cystic BMs, no. (%)	296 (28.1)	50 (29.8)	246 (27.8)
Hemorrhagic BMs, no. (%)	406 (38.5)	58 (34.5)	348 (39.3)
Dural enhancement at BM Dx, no. (%)	248 (23.5)	55 (32.7)	93 (10.5)
Extent of resection, no. (%)*			
GTR	940 (89.4)	142 (85.0)	798 (90.2)
STR	112 (10.6)	25 (15.0)	87 (9.8)
Method of resection, no. (%)*			
Piecemeal	627 (59.6)	112 (67.1)	515 (58.2)
En bloc	425 (40.4)	55 (32.9)	370 (41.8)
Ventricular violation during surgery, no. (%)	21 (2.0)	2 (1.2)	19 (2.1)
Use of CUSA, no. (%)	148 (14.0)	31 (18.5)	117 (13.2)
Mean time to SRS in days	17.32	21.50	41.33
Mean time to WBRT in days	21.84	28.46	20.58
Mean largest BM dimension in mm	31.57	31.65	31.56
Prior radiation, no. (%)	202 (19.2)	33 (19.6)	169 (19.0)
SRS	102 (9.7)	18 (10.7)	84 (9.5)
WBRT	100 (9.5)	15 (8.9)	85 (9.6)
Adjuvant radiation, no. (%)			
SRS	509 (48.3)	99 (58.9)	410 (46.3)
WBRT	424 (40.2)	29 (17.3)	395 (44.6)
Proximity to CSF space, no. (%)			
Separated from CSF space	778 (73.8)	50 (29.7)	528 (59.6)
Contact w/ CSF space	213 (20.2)	79 (47.0)	134 (15.1)
Involved w/ CSF space	60 (5.7)	39 (23.2)	21 (2.4)

CONTINUED ON PAGE 1565 »

» CONTINUED FROM PAGE 1564

TABLE 1. Clinical characteristics of study cohort

Variable	Overall Cohort	LMD Cohort	Control Cohort
Neurological deficits, no. (%)	137 (13.0)	24 (14.3)	113 (12.8)
Median total steroid dose at BM Dx in mg	16.0	14.12	
Steroid tapering, no. (%)	927 (88.0)	151 (89.9)	776 (87.6)
Median KPS score	90	90	90

Dx = diagnosis; KPS = Karnofsky Performance Status; STR = subtotal resection.
* Data were missing for 2 patients (n = 1052).

ed a clear trend toward a decreased LMD risk. An LN metastasis at BM diagnosis (RR 2.38, 95% CI 1.49–3.77, p = 0.001) was associated with a significantly increased risk of LMD (Table 2). This significant association was not observed for extracranial metastases at BM diagnosis (RR 1.10, 95% CI 0.64–1.85, p = 0.70) or with both LN and solid organ metastases (RR 1.50, 95% CI 0.89–2.50, p = 0.12). Breast cancer BM (RR 1.94, 95% CI 1.13–3.33, p = 0.015) was the only BM type that was significantly associated with an increased LMD risk. The receipt of adjuvant radiation was associated with a decreased LMD risk (RR 0.69, 95% CI 0.48–0.98, p = 0.04).

An increased LMD hazard was observed for patients with LN metastases of their primary tumor (hazard ratio [HR] 1.76, 95% CI 1.17–2.65, p = 0.006). Patients with BMs involving the ventricles or pia mater also had an increased LMD hazard (HR 2.17, 95% CI 1.22–3.84, p = 0.008). A cerebral BM location (HR 0.53, 95% CI 0.37–0.74, p = 0.001), GTR of the BM (HR 0.60, 95% CI 0.39–0.94, p = 0.026), en bloc resection (HR 0.68, 95% CI 0.48–0.97, p = 0.033), and the receipt of adjuvant radiation (HR 0.65, 95% CI 0.46–0.92, p = 0.015) were significantly associated with a decreased hazard for LMD (Table 3). Stratified Kaplan-Meier curves of the risk factors mentioned above are visualized in Figures S1–S5. Only LN metastases of the primary tumor at BM diagnosis (adjusted p = 0.015) and cerebellar location (adjusted p = 0.015) were associated with an increased LMD risk after adjustment for multiple testing. A cerebellar BM location was the only independent variable associated with a decreased hazard for LMD (adjusted p = 0.015). Notably, earlier eras of treatment were not significantly associated with an increased risk or hazard for LMD (Tables 2 and 3). Post hoc analysis of the use of PPIs at BM diagnosis revealed no association with an increased LMD risk or hazard. No correlation was observed between steroid use and PPI use at BM diagnosis. The receipt of adjuvant WBRT or SRS was not significantly associated with a decreased LMD risk in the post hoc analysis. Furthermore, no significant associations were observed for the occurrence of nLMD and cLMD (Tables S6 and S7). Univariate subgroup analyses for breast BMs, lung BMs, and melanoma BMs were performed, and the results are presented in Tables S8–S12.

ML Analysis: Prognostication

For the classification task (i.e., the binary occurrence of LMD), an extra trees classifier, XGBoost algorithm, and logistic regression were explored. Discriminatory performance was measured on the hold-out test set with an area under the curve (AUC) between 0.82 and 0.83 for all models. The XGBoost classifier demonstrated the highest discriminatory performance (AUC = 0.83). The most optimal classification models were all trained on a SMOTE ratio of 0.5, that is, a 1:2 ratio of LMD to non-LMD patients after resampling (Table S13). However, the logistic regression model was the best calibrated model compared to the XGBoost and extra trees models, implying the most confident and applicable prediction (Fig. 1). Regression models

TABLE 2. Predictors of LMD occurrence using logistic regression

Variable (ref value)	RR	95% CI	p Value
Primary tumor spread at BM Dx (only BM)	2.38	1.49–3.58	**0.001**
LNs	1.10	0.64–1.85	0.70
Extracranial metastases	1.50	0.89–2.50	0.12
LNs & extracranial metastases			
Cerebral BM location (cerebellar BM location)	0.53	0.37–0.79	**0.001**
Lung BM histology	1.18	0.73–1.92	0.50
Breast BM histology	1.94	1.13–3.33	0.015
Melanoma BM histology	1.16	0.61–2.15	0.70
No. of BMs	1.01	0.96–1.06	0.60
Cystic BM	1.06	0.71–1.55	0.80
Hemorrhagic BM	0.93	0.63–1.35	0.70
Proximity to CSF (separate from CSF space)	1.18	0.75–1.80	0.50
Adjacent to CSF space	1.84	0.92–3.49	0.071
Involved w/ CSF space			
Extent of resection (STR)			
GTR	0.58	0.37–1.03	0.048
Method of resection (piecemeal resection)	0.69	0.47–1.01	0.056
En bloc resection			
Receipt of adjuvant radiation	0.69	0.48–0.98	0.04
Treatment era			
2007–2011	Ref	Ref	Ref
2012–2016	0.68	0.46–1.16	0.1
2017–2019	1.41	0.71–2.66	0.3

A logistic regression was used to explore potential risk factors that influence LMD occurrence in surgically treated BM patients. Values in boldface type are statistically significant at a type I error of 5% after correction using the Holm-Bonferroni method.

TABLE 3. Cox proportional hazards model: risk factors for LMD

Variable (ref value)	HR	95% CI	p Value
Primary tumor spread at BM Dx (only BM)	1.76	1.17–2.65	0.006
LNs	1.10	0.67–1.80	0.70
Extracranial metastases	1.53	0.95–2.46	0.082
LNs & extracranial metastases			
Cerebral BM location (cerebellar BM location)	0.53	0.37–0.74	**0.001**
Lung BM histology	1.01	0.65–1.68	0.90
Breast BM histology	1.21	0.75–1.95	0.40
Melanoma BM histology	0.90	0.51–1.61	0.70
No. of BMs	1.02	0.98–1.06	0.30
Cystic BM	0.98	0.69–1.41	0.90
Hemorrhagic BM	1.14	0.81–1.61	0.50
Proximity to CSF space (separated from CSF space)	1.31	0.89–1.94	0.20
Adjacent to CSF space	2.17	1.22–3.84	0.008
Involved w/ CSF space			
Extent of resection (STR)			
GTR	0.60	0.39–0.94	0.026
Method of resection (piecemeal resection)	0.68	0.48–0.97	0.033
En bloc resection			
Receipt of adjuvant radiation	0.65	0.46–0.92	0.015
Treatment era			
2007–2011	Ref	Ref	Ref
2012–2016	0.87	0.61–1.2	0.4
2017–2019	1.17	0.66–2.07	0.6

A Cox proportional hazards model was used to take time to LMD into account to identify the risk factors that would influence the time to LMD in surgically treated BM patients. Values in boldface type are statistically significant at a type I error of 5% after correction using the Holm-Bonferroni method.

using either a conditional survival forest model or the Cox proportional hazards model were explored to predict the time to LMD. The C-indexes of the best performing models of each algorithm were both 0.76 on the hold-out test set with a SMOTE ratio of 0.5 (Table S14). The 10 most important features included in all the optimal performing models are summarized in Table 4. BM proximity to the ventricles was the most important predictive feature in all models. LN metastasis was the second most important predictive feature for the regression models. Cerebellar location was the second most important feature in two classification models (XGBoost and extra trees classifier). However, the active systemic disease status was the second most important feature in the logistic regression. Interestingly, the use of PPIs at BM diagnosis was included in the 10 most important features for XGBoost and the random forest model, ranked at the ninth and eighth place, respectively.

Discussion

Patients may now live years after the diagnosis of BMs given advances in systemic therapies—particularly targeted therapies and immunotherapies.[34,35] The indications for the resection of BMs include definitive treatment, diagnosis, sampling for molecular testing, and symptomatic relief.[36] However, there are risks to invasive surgery, including increasing the risk of LMD.[3,37] While adjuvant radiation is usually offered after the resection of BMs, it is typically focal and does not address the entire CSF space. The use of craniospinal radiation—radiation delivered to the entire brain and spinal cord CSF spaces—in high-risk scenarios has been attempted with little success.[38]

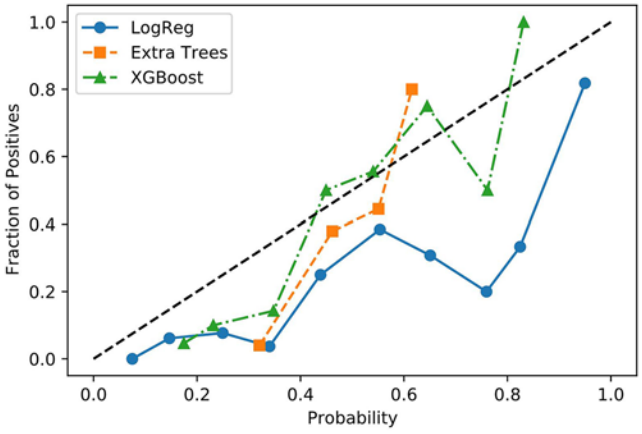

FIG. 1. Calibration plot demonstrating the calibration of all tuned, not fully calibrated classification models. Varying calibration was observed for all classification models, with systematic underestimation observed for the logistic regression (LogReg) model. Figure is available in color online only.

Alternative management strategies such as radiation therapy or systemic therapy may be preferred in certain scenarios. Typically, adjuvant radiation is offered after surgery to increase local control. Because of the known risks for postoperative LMD, there is also growing interest in sequencing radiation prior to surgery to decrease this risk.[39] However, the logistics of coordinating radiation before surgery can be challenging with its own set of risks, such as altered wound healing and an increase in edema and symptoms.[40]

The presented ML models could predict the occurrence of LMD with an AUC of 0.83, the highest discrimination observed in the current literature. In particular, the greatest risk factors or most important features for LMD prognostication were BM proximity to CSF, cerebellar BM location, and systemic LN metastasis at BM diagnosis. Considering these risk factors at the time of surgery may help multidisciplinary oncology teams to best weigh the risks and benefits of resection. Accurate prediction of the postoperative LMD risk has enormous potential to inform clinical decision-making and benefit patients.

Implications

Optimized conventional biostatistical models and ML models performed evenly in this study. The ML models offer more insight into the relationships between independent variables in a personalized nonlinear manner. ML could also help to alleviate spurious findings due to the nonlinearity of data and may become increasingly important as bigger data sets are curated. The diagnosis-specific

TABLE 4. Feature importance list for optimized performance for all ML models

Feature No.	XGBoost	Extra Trees Classifier	Logistic Regression	Random Forest	Cox Model
1	Proximity to CSF space	Proximity to CSF space	Proximity to CSF space	Proximity to CSF space	Proximity to CSF space
2	Cerebellar BM location	Cerebellar BM location	Active systemic disease status	Extracranial metastasis	Extracranial metastasis
3	Hemorrhagic BMs	Breast carcinoma	Hemispheric BM location	Cerebellar BM location	Gynecological carcinoma
4	Piecemeal resection	Piecemeal resection	Use of steroids	No. of BMs at Dx	Use of steroids
5	Active systemic disease status	Sex	Breast carcinoma	Hemispheric BM location	Active systemic disease status
6	Sex	Cystic BMs	Lung carcinoma	Sex	Colorectal carcinoma
7	Renal carcinoma	Primary tumor spread	Use of CUSA	Piecemeal resection	No. of BMs at Dx
8	Breast carcinoma	Active systemic disease status	Colorectal carcinoma	PPI use at BM Dx	Prior SRS or WBRT
9	PPI use at BM Dx	STR	Neurological deficits at BM Dx	Lung carcinoma	Time from BM Dx to SRS
10	KPS	Hemispheric BM location	Prior SRS or WBRT	Hemorrhagic BMs	Hemorrhagic BMs

Proximity to CSF spaces combined with cerebellar location, the presence of extracranial metastasis, and active systemic primary malignancies were the most important features. The importance of features is determined by the frequency with which features appear in the learning or optimization of models on training data. The features must be looked at holistically, that is, combined with the other features in the list, and cannot be isolated for inferences.

graded prognostic assessment[41] and its adaptations[42] are the gold standard for survival prognostication of newly diagnosed BM patients stratified by their primary tumor location. The highest achieved C-index of the regression models mentioned above was 0.604 on externally validated data. The performance metrics on the hold-out test set of our LMD data set were optimized to 0.76 for the time to LMD prognostication and 0.83 for LMD classification. Therefore, one can conclude that less common phenomena, such as LMD, can be feasibly prognosticated.

The most important feature in the ML analysis was BM proximity to the CSF space, followed by a cerebellar BM location. Expressly, features on the importance list should not be interpreted independently in contrast to inferential analysis; all features combined accumulate to an estimated probability of (time to) LMD occurrence. The use of PPIs at BM diagnosis was listed as an important feature for two models. Nevertheless, it did not have an association with (time to) LMD. This finding may be spurious, although it has been observed that PPI use decreases overall survival in lung cancer patients who have received targeted therapy concurrently.[43]

In this study, we observed LMD risk factors that were previously suspected of having an association with LMD risk in small data sets. An increased LMD risk has been observed in the medical literature for cerebellar BMs,[29] piecemeal resections,[3] or BMs that were subtotally resected.[30] One previous study reported that BMs that were either adjacent to or involved with the ventricles were associated with an increased LMD risk.[3] An increased LMD risk and shortened time to LMD in that study were also observed for patients with BMs involving the ventricles.[3]

Breast cancer histology was the only primary tumor type associated with an increased LMD risk, which is in line with findings in the current medical literature.[29] The large number of patients included in our study and the similar associations made in previous smaller studies give us more confidence in the associations listed above. Contrasting results regarding HER2 status in breast cancer BM patients have been reported to date.[3,31,33] In the subgroup analysis for breast cancer BM patients, HER2-positive breast cancer BMs were not associated with a significant effect on LMD risk—although this may be an effect of improving HER2-directed systemic therapies in our cohort from the time of prior reports.

One of the strongest LMD risk factors in our study was a cerebellar BM location, as previously identified in the medical literature.[29] The cerebrum has distinct gyri and sulci, which help to distinguish tumor from brain tissue and may help to avoid CSF space violation intraoperatively. In contrast, the dense folia of the cerebellum make intraoperative CSF contamination likelier.

LN metastasis as a risk factor for LMD is a novel finding of our study, and to our knowledge, this association has not been previously described in the literature. Across statistical models, we consistently found LN metastasis to be a highly important risk feature. Interestingly, LN metastases of the primary tumor at BM diagnosis were associated with an increased LMD risk and a shorter time to LMD regardless of the presence of solid organ metastases at BM diagnosis. There are growing data that lymphatic pathways may provide entry into the CSF spaces. Recent in vivo animal studies have shown that lymphatic vessels of the meninges drain on the deep cervical nodes, where the systemic immune response could be initiated on presented brain parenchymal antigens.[44,45] This pathway bypasses the blood-brain barrier and hypothetically forms an access point to the brain. Our results suggest an important role for the lymphogenic spread of primary tumor in the occurrence of LMD. While this may be a function of more aggressive overall disease, our understanding of lymphatic and therefore immunological interactions with the brain is in its infancy and has enormous implications with regard to new immunotherapies such as chimeric antigen receptor (CAR) T-cell therapy.

Study Limitations

Patients in this study encompassed a wide period (2007–2019) during which there were tremendous advanc-

es in surgical technique as well as radiation and systemic therapies. However, LMD risk or hazard was not significantly associated with one specific period. Furthermore, radiographic elements, such as cystic and hemorrhagic BM components, were only classified as such if they were deemed clinically relevant by radiologists. Future research could focus on the isolated role of these radiographic components in LMD, regardless of the clinical relevancy or size of the radiographic component. Additionally, LN metastasis as an LMD risk factor is a novel finding. Future (prospective) studies can focus further on the presence of LN metastases in certain locations, such as deep cervical LN metastases, and their potential relation to LMD. The data used in this study represent only the neurosurgically resected BMs, as our hypothesis was that surgical treatment increased LMD incidence due to surgical spillage. Therefore, BM patients receiving only radiation therapy were excluded from this study. Comparing these patients could enhance our understanding of the added risk of resection over inherent tumor risks. The use of SMOTE to handle the inherent class imbalance of this data set also reduces the variability of the presented data. To date, over- or undersampling methods are the only options to build prediction models for less common phenomena, such as LMD. Our study aim was to demonstrate the feasibility of LMD prediction based on patient, tumor, and treatment characteristics; however, LMD prognostication at BM diagnosis in clinical care remains a theoretical ideal for the time being. The next step would be to externally validate our models using independent data to assess the generalizability of the models. Furthermore, LMD risk factors reported in the current literature were verified through the presented large data set, and possible novel LMD risk factors, such as LN metastases of the primary tumor, were explored.

Conclusions

LMD prognostication using SMOTE and ML algorithms is feasible despite the disease's low prevalence in the BM population. LN metastasis of the primary tumor at BM diagnosis and a cerebellar BM location were the strongest risk factors for LMD. Other risk factors that influence LMD occurrence are proximity of the BMs to CSF spaces, method of resection, and extent of resection. Future efforts should focus on further understanding LMD prediction in the setting of modern systemic therapies.

References

1. Lee S, Ahn HK, Park YH, et al. Leptomeningeal metastases from breast cancer: intrinsic subtypes may affect unique clinical manifestations. *Breast Cancer Res Treat*. 2011; 129(3):809-817.
2. Winn HR. *Youmans Neurological Surgery*. WB Saunders; 2004.
3. Ahn JH, Lee SH, Kim S, et al. Risk for leptomeningeal seeding after resection for brain metastases: implication of tumor location with mode of resection. *J Neurosurg*. 2012;116(5): 984-993.
4. Suki D, Abouassi H, Patel AJ, Sawaya R, Weinberg JS, Groves MD. Comparative risk of leptomeningeal disease after resection or stereotactic radiosurgery for solid tumor metastasis to the posterior fossa. *J Neurosurg*. 2008;108(2): 248-257.
5. Siomin VE, Vogelbaum MA, Kanner AA, Lee SY, Suh JH, Barnett GH. Posterior fossa metastases: risk of leptomeningeal disease when treated with stereotactic radiosurgery compared to surgery. *J Neurooncol*. 2004;67(1-2):115-121.
6. Le Rhun E, Taillibert S, Chamberlain MC. Carcinomatous meningitis: leptomeningeal metastases in solid tumors. *Surg Neurol Int*. 2013;4(suppl 4):S265-S288.
7. Oechsle K, Lange-Brock V, Kruell A, Bokemeyer C, de Wit M. Prognostic factors and treatment options in patients with leptomeningeal metastases of different primary tumors: a retrospective analysis. *J Cancer Res Clin Oncol*. 2010;136(11): 1729-1735.
8. Park JH, Kim YJ, Lee JO, et al. Clinical outcomes of leptomeningeal metastasis in patients with non-small cell lung cancer in the modern chemotherapy era. *Lung Cancer*. 2012; 76(3):387-392.
9. Tan Y, Mu W, Wang XC, Yang GQ, Gillies RJ, Zhang H. Improving survival prediction of high-grade glioma via machine learning techniques based on MRI radiomic, genetic and clinical risk factors. *Eur J Radiol*. 2019;120:108609.
10. Senders JT, Staples P, Mehrtash A, et al. An online calculator for the prediction of survival in glioblastoma patients using classical statistics and machine learning. *Neurosurgery*. 2020;86(2):E184-E192.
11. Cho SJ, Sunwoo L, Baik SH, Bae YJ, Choi BS, Kim JH. Brain metastasis detection using machine learning: a systematic review and meta-analysis. *Neuro Oncol*. 2021;23(2): 214-225.
12. Le Rhun E, Guckenberger M, Smits M, et al. EANO-ESMO Clinical Practice Guidelines for diagnosis, treatment and follow-up of patients with brain metastasis from solid tumours. *Ann Oncol*. 2021;32(11):1332-1347.
13. Turner BE, Prabhu RS, Burri SH, et al. Nodular leptomeningeal disease—a distinct pattern of recurrence after postresection stereotactic radiosurgery for brain metastases: a multi-institutional study of interobserver reliability. *Int J Radiat Oncol Biol Phys*. 2020;106(3):579-586.
14. Prabhu RS, Turner BE, Asher AL, et al. Leptomeningeal disease and neurologic death after surgical resection and radiosurgery for brain metastases: a multi-institutional analysis. *Adv Radiat Oncol*. 2021;6(2):100644.
15. McHugh ML. Interrater reliability: the kappa statistic. *Biochem Med (Zagreb)*. 2012;22(3):276-282.
16. Kancharla P, Ivanov A, Chan S, Ashamalla H, Huang RY, Yanagihara TK. The effect of brain metastasis location on clinical outcomes: a review of the literature. *Neurooncol Adv*. 2019;1(1):vdz017.
17. Lin NU, Lee EQ, Aoyama H, et al. Response assessment criteria for brain metastases: proposal from the RANO group. *Lancet Oncol*. 2015;16(6):e270-e278.
18. Staartjes VE, Schröder ML. Class imbalance in machine learning for neurosurgical outcome prediction: are our models valid? Letter. *J Neurosurg Spine*. 2018;29(5):611-612.
19. Chawla NV, Bowyer KW, Hall LO, Kegelmeyer WP. SMOTE: Synthetic Minority Over-sampling Technique. *J Artif Intell Res*. 2002;16:321-357.
20. R: A language and environment for statistical computing. R Foundation for Statistical Computing. Accessed September 12, 2022. https://www.R-project.org
21. Python Language Reference, version 3.9.5. Python Software Foundation. Accessed September 12, 2022. https://www.python.org
22. Pedregosa F, Varoquaux G, Gramfort A, et al. Scikit-learn: machine learning in Python. *J Mach Learn Res*. 2011;12: 2825-2830.
23. Peng H, Long F, Ding C. Feature selection based on mutual information: criteria of max-dependency, max-relevance,

and min-redundancy. *IEEE Trans Pattern Anal Mach Intell*. 2005;27(8):1226-1238.
24. Steyerberg EW, Vickers AJ, Cook NR, et al. Assessing the performance of prediction models: a framework for traditional and novel measures. *Epidemiology*. 2010;21(1):128-138.
25. Nguyen TK, Sahgal A, Detsky J, et al. Predictors of leptomeningeal disease following hypofractionated stereotactic radiotherapy for intact and resected brain metastases. *Neuro Oncol*. 2020;22(1):84-93.
26. Foreman PM, Jackson BE, Singh KP, et al. Postoperative radiosurgery for the treatment of metastatic brain tumor: evaluation of local failure and leptomeningeal disease. *J Clin Neurosci*. 2018;49:48-55.
27. DePaoli B, Gozal YM, Pater LE, et al. Ventricular violation increases the risk of leptomeningeal disease in cavity-directed radiosurgery treated patients. *J Radiat Oncol*. 2019; 8:23-29.
28. Keller A, Doré M, Cebula H, et al. Hypofractionated stereotactic radiation therapy to the resection bed for intracranial metastases. *Int J Radiat Oncol Biol Phys*. 2017;99(5):1179-1189.
29. Ojerholm E, Lee JY, Thawani JP, et al. Stereotactic radiosurgery to the resection bed for intracranial metastases and risk of leptomeningeal carcinomatosis. *J Neurosurg*. 2014; 121(suppl):75-83.
30. Soliman H, Myrehaug S, Tseng CL, et al. Image-guided, linac-based, surgical cavity-hypofractionated stereotactic radiotherapy in 5 daily fractions for brain metastases. *Neurosurgery*. 2019;85(5):E860-E869.
31. Atalar B, Modlin LA, Choi CY, et al. Risk of leptomeningeal disease in patients treated with stereotactic radiosurgery targeting the postoperative resection cavity for brain metastases. *Int J Radiat Oncol Biol Phys*. 2013;87(4):713-718.
32. Patel KR, Burri SH, Asher AL, et al. Comparing preoperative with postoperative stereotactic radiosurgery for resectable brain metastases: a multi-institutional analysis. *Neurosurgery*. 2016;79(2):279-285.
33. Press RH, Zhang C, Chowdhary M, et al. Hemorrhagic and cystic brain metastases are associated with an increased risk of leptomeningeal dissemination after surgical resection and adjuvant stereotactic radiosurgery. *Neurosurgery*. 2019;85(5): 632-641.
34. Bartsch R, Berghoff A, Pluschnig U, et al. Systemic therapy and overall survival (OS) in patients (pts) with brain metastases from HER2-positive (HER2+) metastatic breast cancer (MBC). *J Clin Oncol*. 2011;29(15 suppl):597.
35. Rick JW, Shahin M, Chandra A, et al. Systemic therapy for brain metastases. *Crit Rev Oncol Hematol*. 2019;142:44-50.
36. Graber JJ, Cobbs CS, Olson JJ. Congress of Neurological Surgeons systematic review and evidence-based guidelines on the use of stereotactic radiosurgery in the treatment of adults with metastatic brain tumors. *Neurosurgery*. 2019; 84(3):E168-E170.
37. van der Ree TC, Dippel DW, Avezaat CJ, Smitt PAS, Vecht CJ, van den Bent MJ. Leptomeningeal metastasis after surgical resection of brain metastases. *J Neurol Neurosurg Psychiatry*. 1999;66(2):225-227.
38. Maillie L, Salgado LR, Lazarev S. A systematic review of craniospinal irradiation for leptomeningeal disease: past, present, and future. *Clin Transl Oncol*. 2021;23(10):2109-2119.
39. Prabhu RS, Dhakal R, Vaslow ZK, et al. Preoperative radiosurgery for resected brain metastases: the PROPS-BM multicenter cohort study. *Int J Radiat Oncol Biol Phys*. 2021; 111(3):764-772.
40. Diehl CD, Shiban E, Straube C, et al. Neoadjuvant stereotactic radiosurgery for intracerebral metastases of solid tumors (NepoMUC): a phase I dose escalation trial. *Cancer Commun (Lond)*. 2019;39(1):73.
41. Sperduto PW, Kased N, Roberge D, et al. Summary report on the graded prognostic assessment: an accurate and facile diagnosis-specific tool to estimate survival for patients with brain metastases. *J Clin Oncol*. 2012;30(4):419-425.
42. Barnholtz-Sloan JS, Yu C, Sloan AE, et al. A nomogram for individualized estimation of survival among patients with brain metastasis. *Neuro Oncol*. 2012;14(7):910-918.
43. Fang YH, Yang YH, Hsieh MJ, Hung MS, Lin YC. Concurrent proton-pump inhibitors increase risk of death for lung cancer patients receiving 1st-line gefitinib treatment—a nationwide population-based study. *Cancer Manag Res*. 2019; 11:8539-8546.
44. Hu X, Deng Q, Ma L, et al. Meningeal lymphatic vessels regulate brain tumor drainage and immunity. *Cell Res*. 2020; 30(3):229-243.
45. Ma Q, Schlegel F, Bachmann SB, et al. Lymphatic outflow of cerebrospinal fluid is reduced in glioma. *Sci Rep*. 2019;9(1): 14815.

Disclosures

The authors report no conflict of interest concerning the materials or methods used in this study or the findings specified in this paper.

Author Contributions

Conception and design: Tewarie, Hulsbergen, Phillips. Acquisition of data: Tewarie, Jessurun, Zhang, Hulsbergen, Rendon, McNulty. Analysis and interpretation of data: Tewarie, Senko. Drafting the article: Tewarie, Senko. Critically revising the article: Tewarie, Jessurun, Broekman, Smith, Phillips. Reviewed submitted version of manuscript: Tewarie, Senko, Jessurun, Broekman, Peng, Phillips. Approved the final version of the manuscript on behalf of all authors: Tewarie. Statistical analysis: Tewarie, Senko. Study supervision: Broekman, Peng, Smith, Phillips.

Supplemental Information

Online-Only Content

Supplemental material is available with the online version of the article.

Figs. S1–S5 and Tables S6–S14. https://thejns.org/doi/suppl/10.3171/2022.8.JNS22744.

Correspondence

Ishaan Ashwini Tewarie: Brigham and Women's Hospital, Harvard Medical School, Boston, MA. ishaantewarie@gmail.com.